Organic & Biomolecular Chemistry

Accepted Manuscript

This article can be cited before page numbers have been issued, to do this please use: S. Bujosa, E. Castellanos, A. Frontera, C. Rotger, A. Costa and B. Soberats, *Org. Biomol. Chem.*, 2020, DOI: 10.1039/C9OB02085C.

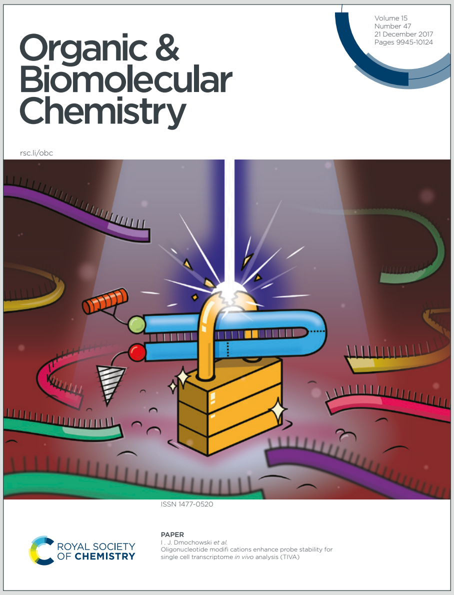

Organic & Biomolecular Chemistry

Volume 15
Number 47
21 December 2017
Pages 9945-10124

rsc.li/obc

ISSN 1477-0520

ROYAL SOCIETY OF CHEMISTRY

PAPER
I . J. Dmochowski *et al.*
Oligonucleotide modifi cations enhance probe stability for single cell transcriptome *in vivo* analysis (TIVA)

ROYAL SOCIETY OF CHEMISTRY

rsc.li/obc

View Article Online
DOI: 10.1039/C9OB02085C

ARTICLE

Self-assembly in water of amphiphilic aryl-squaramides driven by dipolar π–π interactions

Received 00th January 20xx,
Accepted 00th January 20xx

DOI: 10.1039/x0xx00000x

Sergi Bujosa,[a] Eduardo Castellanos,[a] Antonio Frontera,[a] Carmen Rotger,[a] Antonio Costa*[a] and Bartolome Soberats*[a]

Squaramides are versatile compounds with a great capacity to interact *via* non-covalent interactions and therefore of interest for the development of supramolecular systems and functional materials. In the present work, a new series of aryl-squaramides amphiphiles (**1-5**) were prepared to form supramolecular polymers in water. Interestingly, only compounds **1** and **2**, that contain electron-deficient aryl groups are capable of forming hydrogels (~10^{-2} M) upon treatment with base (NaOH or PBS). The aggregation behaviour of **1** and **2** was studied by static light scattering, UV-Vis, ^{1}H NMR, FT-IR, and atomic force microscopy, and it was found that these compounds aggregate forming well-defined 1D nanofibers below the critical gelation concentration (<10^{-3} M). Moreover, the combination of those experiments with 1D and 2D NMR studies and theoretical calculations revealed that **1** and **2** self-assemble *via* an unprecedented interaction motif consisting of dipolar π–π interactions between the squaramide rings and the 4-nitrophenyl or 3,5-bis(trifluromethyl)phenyl rings of **1** and **2**, respectively. Such kind of assemblies are stabilized by the compensation of the dipole moments of the stacked molecules. This interaction mode contrasts with those typically driving squaramide-based assemblies based on hydrogen bonds or either by antiparallel stacking. We believe that this interaction motif is of interest for the design and development of new squaramide nanomaterials with free hydrogen bonding groups, which might be useful in drug delivery applications.

Introduction

Supramolecular polymers are attracting a great deal of attention due to its potential in material science and chemical biology.[1-13] Thus, many efforts have been addressed to develop new molecular design strategies to prepare monomers that self-assemble forming specific nanostructures and in turn, exhibit the desired functions. This task is specially challenging when water is used as solvent and the hydrophobic effects are dominating the assembly processes.[14-19] While the simplest surfactants, based on aliphatic chains functionalized with ionic heads, self-assemble forming micelles or vesicles, the utilization of alternative molecular structures are required to develop more complex functional structures in water.[14-19] For these purposes it is necessary to design molecules with specific functional groups that can direct the self-assembly processes *via* additional weak and reversible non-covalent interactions such as hydrogen bonds[20-24] (H-bonds) or π–π interactions.[25-33]

Amphiphilic π-extended aromatic scaffolds have been widely exploited to create complex supramolecular architectures in water *via* π–π interactions.[25-33] For example, Lee and coworkers extensively studied the molecular design of π-extended amphiphiles in order to obtain aggregates with different morphologies *i.e.* fibers, toroids, tubes, etc. that in turn exhibit stimuli responsive optoelectronic and photonic properties.[29,30] However, despite π–π interactions are strong in aqueous environments, they are not directional and the resulting assemblies often suffer of translational and rotational freedom which prevents higher level of structural control. Other kind of interactions such as charge transfer complexes (donor-acceptor) or dipole-dipole π–π-interactions can provide additional directional control over the assemblies.[34-40] For example, the group of Ghosh studied the self-assembly by the alternate stacking of electron poor and electron rich aromatic scaffolds as strategy to build multicomponent assemblies.[24-36] On the other hand, Würthner and co-workers focused on the self-assembly studies of merocyanine dyes through dipole-dipole interactions in low polarity environments.[37-40] Such specific and directional π–π interactions are proved to offer additional control on the aggregates and therefore could be utilized in water systems for the further development of novel functional aqua materials.[14-19]

In the present work, we unveil two aryl-squaramide systems that aggregate in water *via* hydrophobic effects and dipolar π–π interactions to form fibrous supramolecular aggregates and hydrogels. This interaction motif was discovered thought the exploration of aryl-squaramides **1-5** (Fig. 1a) as new hydrogel materials. However, it was found that only **1** and **2**, bearing electron-deficient aryl groups, form fibrillar supramolecular aggregates (at lower concentrations) and hydrogels (at higher concentrations) under the appropriate conditions (pH=7-8).

---

[a] *Universitat de les Illes Balears, Crta. de Valldemossa Km 7.5, 07122 Palma de Mallorca, Spain.*

† Electronic Supplementary Information (ESI) available: [Experimental methods, synthetic procedures, NMR experiments, AFM, UV-Vis experiments, FT-IR experiments and theoretical studies]. See DOI: 10.1039/x0xx00000x

View Article Online
DOI: 10.1039/C9OB03085G

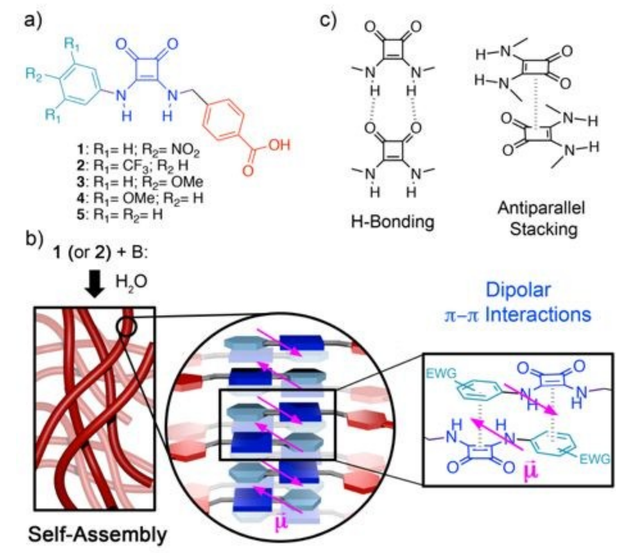

Fig. 1. Molecular structure of aryl squaramides **1-5**. b) Schematic representation of the self-assembly in water of compound **1** and **2** *via* dipolar π–π interactions. Electron withdrawing groups (EWG); Base (B:); dipole moment (μ) is represented as pink arrows. c) Common interaction modes of squaramides *via* quadruple H-bonds (left) and antiparallel stacking (right).

Interestingly, NMR, UV-Vis, and FT-IR, as well as theoretical calculations, permitted to conclude that **1** and **2** self-assemble *via* dipolar π–π interactions by the cancellation of the dipole moments (μ) between vicinal molecules as shown in Fig. 1b. This interaction motif contrasts with the common interaction modes of squaramides consisting of H-bonds[41-46] or antiparallel stacking (Fig. 1c)[47-49] and opens new possibilities for the design and development of squaramide assemblies[50] with free NH positions as H-bonding acceptors.

Results and discussion

Molecular design and hydrogels formation

The molecular design of the new squaramides **1-5** was inspired by our previously described materials **Sq(NO$_2$)** and **Sq(CF$_3$)** consisting of an arylsquaramide with an appended benzylsquaramate group (Fig. S1).[51] These compounds form thixotropic hydrogels and were found to be useful for the controlled-release of organic molecules in water. Initially, we thought that those compounds would associate by H-bonds or either by antiparallel stacking as it is well-known in squaramides.[41-50] For example, we previously reported a tripodal receptor bearing three squaramide groups that forms 1D nanofibres in CHCl$_3$ *via* H-bonding interactions.[41] Similar supramolecular polymers were obtained in water using squaramide amphiphiles by H-bonds reinforced by an aromatic gain.[44,45] However, we could not find enough evidence about the interaction mode for **Sq(NO$_2$)** and **Sq(CF$_3$)** hydrogels due to the strong interactions involved in the system.[51] In the present work, we designed the next generation of aryl-squaramide hydrogels bearing a benzoic acid group (Fig. 1a). We expected to decrease the aggregation tendency by replacing the benzyl-squaramate group for a benzoate group since the squaramate moiety provide to the molecule a highly ionizable group, an aromatic system and a H-bond donor group from which it can be built several intermolecular interations while the carboxylate gives only an moderate ionisable group. We reckoned that the structural modification would permit to study the aggregation features in more detail. For building the new series of compounds, we selected five different aryl groups to incorporate at the squaramidic end of the molecule in order to tune the material properties. Thus, the compounds bear 4-nitrophenyl (**1**), 3,5-(bis(trifluoromethane))phenyl (**2**), 4-methoxyphenyl (**3**), 3,5-dimethoxyphenyl (**4**) and phenyl (**5**) rings. Squaramides **1-5** were prepared easily in a two steps process involving the formation of the corresponding aryl-squaramide esters and followed by the condensation with 4-(aminomethyl)benzoic acid. For synthetic details see the ESI†, Scheme S1, and Figures S2-S11.

Hydrogels based on compounds **1**-**5** were prepared according to our previously described procedure,[51] consisting on heating (80-90 °C) the insoluble squaramide compounds (1.0 wt%) in a basic water solution (NaOH or phosphate buffer (PBS), pH 7-8), followed by slow cooling of the samples (see Experimental section). This process warrants the total deprotonation of the benzoic acid (pK$_a$= 4.2) group and facilitates the solubilization of compounds **1-5** at high temperatures (Fig. 2a). We observed that after the slow cooling

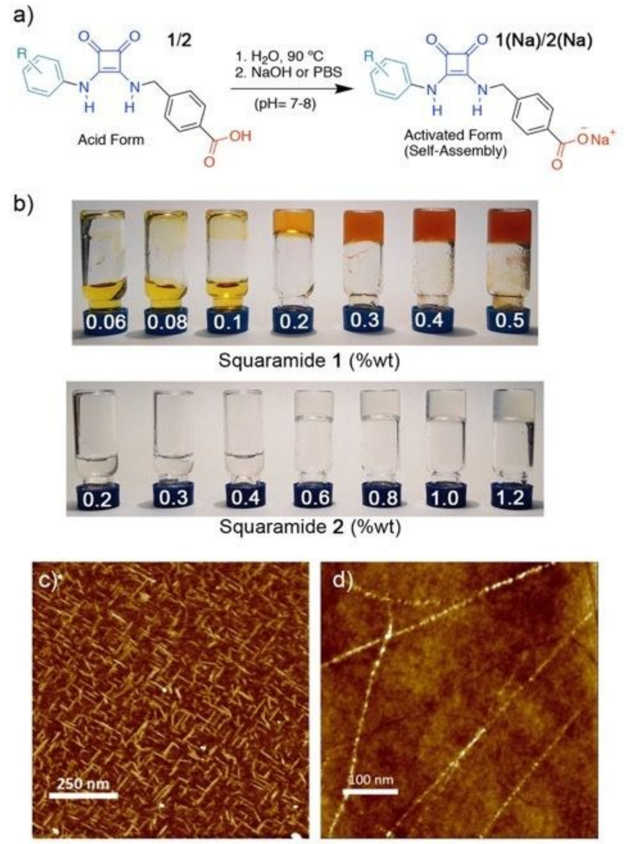

Fig. 2. a) Scheme of the deprotonation of the benzoic acid group of **1** and **2** upon treatment with NaOH or PBS. b) Inversion test of the vials with compounds **1** (top) and **2** (bottom) at different concentrations (% wt) after treatment with PBS (pH=7-8). AFM images of spin coated solutions (1.0 × 10^{-4} M, PBS) of c) **1** and d) **2** on mica substrates

View Article Online
DOI: 10.1039/C9OB02085C

of the samples, compounds **1** and **2** form gels (Fig. 2b), while compounds **3-5** precipitate in powder form. It is noteworthy that compounds **1** and **2** are the only ones of the series that bear electron-withdrawing groups in the aryl rings. Additional pH dependent UV-Vis experiments indicate that compounds **1** and **2** do not suffer the deprotonation of the first squaramidic NHs until pHs higher than 9 (Fig. S19).[52,53] Fig. 2b shows the inversion tests of the vials containing samples of **1** (top) and **2** (bottom) at different concentrations after the basic treatment in PBS at high temperatures. In the case of **1** the approximate critical gelation concentration (CGCs) is 0.2 wt%, while it is required 0.6 wt% of compound **2** to form self-consistent hydrogels. The sol-gel transition temperatures for both **1** (0.6 wt%, PBS) and **2** (1 wt%, PBS) hydrogels were estimated to be around 65 °C, according to the variable temperature NMR experiments (Figs. S16 and S17). Rheology experiments of the hydrogels prepared in NaOH were also measured and are shown in Fig. S18. These results suggest that compounds **1** and **2** form specific assemblies suitable for the formation of firm hydrogels.

To observe in detail the morphology of the aggregates, PBS solutions of **1** and **2** below the CGC (*ca.* 1×10^{-4} M) were spin-coated on mica substrates and were analysed by AFM (Figs. 2c, S12, and S13). Fig. 2c shows the AFM image of the spin-coated solution of **1** (1×10^{-4} M) that evidences the formation of rigid fibers of 18 nm of width and 0.4 nm of thickness (Fig. S12). Compound **2** (1×10^{-4} M) also aggregates forming fibrillar structures, but in this case the fibers are longer and less rigid tending to form helical structures (Figs. 2d and S13). These results confirm the aggregation of compounds **1** and **2** into fibrillar nanostructures which enables at higher concentration the formation of networks and subsequently hydrogels (Fig. 2b).[51,54-57]

Aggregation studies

The aggregation behaviour in solution of compounds **1** and **2** was then analysed by Static Light Scattering (SLS), ^{1}H NMR, FT-IR, and UV-Vis experiments. First, we analysed the scattered intensities (SLS experiments) of **1** and **2** in PBS (pH=7-8) as a function of the concentration (Fig. 3a).‡ We found that the intensities of the scattered light increas after reaching certain concentration, as result of the aggregation of the systems. From the experimental data, we could calculate the critical aggregation concentrations (CACs) for **1** and **2** to be 3.3×10^{-4} M and 3.7×10^{-4} M, respectively (Fig. 3a). The formation of aggregates was further supported by running variable concentration NMR experiments. The ^{1}H NMR spectra of **1** and **2** exhibit broad signals at concentrations of 1-2 $\times10^{-2}$ M, while the signals become sharper at lower concentrations around 1×10^{-4} M (Figs. S14 and S15). This sharpening of the NMR signals by decreasing concentration was attributed to the system de-aggregation.[5]

To get more details about the aggregation process, concentration dependent UV-Vis studies of **1** and **2** were carried out in PBS. The UV-Vis spectrum of **1** in PBS shows two main broad bands at 385 and 280 nm (Fig. 3b) which correspond to electronic transitions of the 4-nitrophenyl and squaramide parts, respectively (Fig. S20). Similar spectral profile is observed for **2** and shows two bands at 325 and 280 nm (Fig. S21). It is noteworthy that the bands corresponding to the aryl groups of **1** and **2** are batochromically shifted 100 and 60 nm compared to the N-(4-nitrophenyl)acetamide and N-(3,5-bis(trifluoromethyl)phenyl)acetamide bands (Figs. S20, S21, respectively, which suggest the extension of the aryl π system towards the squaramide ring.[44,58,59] Variable concentration experiments of compound **1** revealed a marked hypochromic (overall decrease of the molar absorption coefficient) effect upon increasing concentration (Figs. 3b and S22) between 2.0×10^{-4} M and 2.5×10^{-3} M which is the same concentration range of the CAC calculated from the SLS studies. This effect is accompanied by slight blue-shift of the band at 385 nm. Compound **2** also exhibits analogous hypochromic effect in the concentration range between 1×10^{-5} and 5×10^{-3} M as shown in Fig. S23. The hypochromic effect is attributed to an aggregation process and indicates a relatively broad distribution of translational and rotational displacements between molecules in the aggregates suggesting that the molecules are not highly constrained within the assembly.[60,61] The experimental data points of the concentration dependent UV-Vis experiments were fitted to the nucleation-elongation aggregation model.[62] While compound **2** could be fitted to the cooperative model (Fig. S23), the experimental points of compound **1** did not fit (Fig. S22) to this model, probably due to the gelification/precipitation of the sample during the elongation process.§

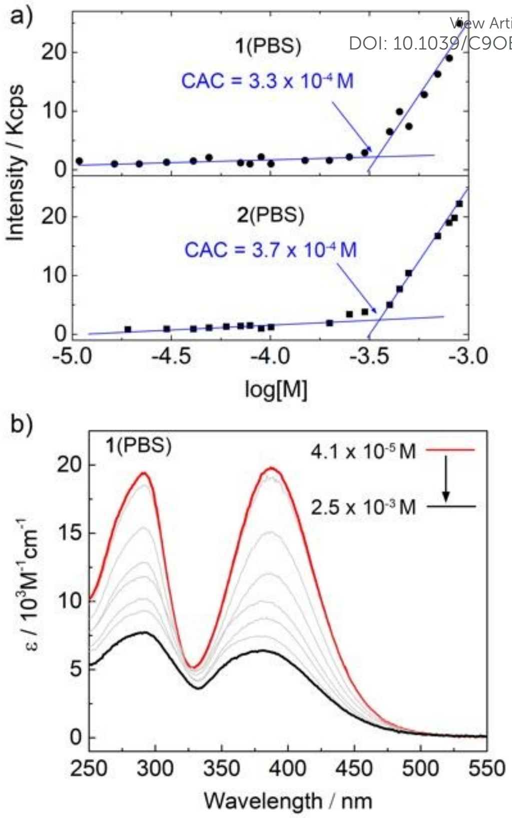

Fig, 3. a) Scattered intensity (s^{-1}) as function of the concentration (log[M]) of **1** (top) and **2** (bottom) in PBS. Inset is shown the CAC. b) UV-Vis spectra of **1** in PBS at different concentrations

The SLS and UV-Vis experiments point out that compounds **1** and **2** self-assemble at relatively high concentrations and the resulting aggregates are not very strong and undergo molecular displacements. These features are not consistent with an assembly based on H-bonds (Fig. 1c).[41-45] Indeed, Kieltyka and co-workers previously reported on H-bonded squaramide amphiphiles forming well-defined fibers in water.[44-45] They described that, upon aggregation, two sharp UV-Vis bands at 255 and 328 nm appear while the monomer exhibits a single band around 300 nm. The appearance of these two bands is indicative of the formation of H-Bonds between squaramides.[44-45] However, these bands do not appear in the UV-Vis spectra of **1** and **2** even at high concentrations where the molecules are highly aggregated (Figs S20-S23). To discard the formation of H-bonds, we prepared **1** and **2** xerogels (PBS) and analysed them by IR spectroscopy (Figs S24,S25). The FT-IR spectra of hydrogels **1** and **2** show two sharp bands at 1796 cm^{-1} and 1693 cm^{-1}, and 1799 cm^{-1} and 1692 cm^{-1} respectively. These peaks correspond to the squaramide breathing and the CO stretching.[44,45,63] Above 3000 cm^{-1} appear the bands corresponding to phosphate groups and water at 3086, 3128, 3385 and 3448 cm^{-1} (Fig. S26). However, no bands are observed between 3128 and 3385 cm^{-1}, where usually the stretching of H-bonded squaramidic NHs appears. Figs S24,S25).[44] This observation supports that the the squaramidic compounds are not H-bonded and the NH stretching signals are probably below the broad band between 3384 and 3500 cm^{-1}.

To learn more about the parts of the molecules involved in the self-assembly process, ^1H NMR experiments of **1(Na)** and **2(Na)**[§§] (see Experimental part) in DMSO-*d6*/H_2O mixtures were carried out at 1.0×10^{-3} M (Figs. 4a-b and S27). It was assumed that both compounds are highly aggregated in water at these concentrations, while they are monomerically dissolved in DMSO-*d6*.[51] Interestingly, we could observe that the aromatic ^1H NMR signals of **1** and **2** in H_2O/DMSO-*d6* mixtures show significant shifts upon increasing the ratio of H_2O (Fig. 4b and S27). The NMR signals of frotons H_a, H_c and H_d (Fig. 4a) of compound **2** undergo first a deshielding and then a shielding upon increasing the ratio of water. On the other hand, the H_b proton of the 3,5-(bis(trifluoromethane))phenyl ring of **2** appears at 8.7 ppm in pure DMSO and is shifted up to 7.7 ppm in a 5:95 DMSO-*d6*/H_2O mixture (Fig. 4b). These shifts of the aromatic signals were attributed to a conformational change of the molecules and the concomitant shielding resulting from the aggregation *via* π–π interactions in the water mixtures. It is noteworthy that these experiments show no signals of the squaramidic NHs in the presence of any ratio of water. This supports our assumption that **1** and **2** are not forming H-bonds and therefore the squaramidic NH groups that are not shielded into the aggregates can exchange protons with the aqueous medium.

More precise information about the molecular environments in the **1** and **2** aggregates was obtained by 2D NMR NOESY experiments in D_2O and in DMSO-*d6* (Figs 4c and S28-S42). Fig. 4c shows the relevant part of the NOESY spectrum of **2** in D_2O/NaOD, where NOE contacts between the aryl protons H_a and H_b with the methylene protons (H_{CH2}) (Fig. 4a) are observed. Similar results were obtained by using PBS (Figs. S35-S38). These NOE signals indicate the proximity in the space of these protons, which can only be the result of intermolecular proximities in the aggregated structure. This is supported by the fact that no NOE signals are observed for **2(Na)** between those protons in DMSO-*d6* in the monomeric state (Fig. S41 and S42). Analogous results were found for compound **1** (Figs S28, S29, S31-S34, S39, S40), where NOE signals are observed between the protons of the nitrobenzene ring and the CH_2 in aqueous solutions.

View Article Online
DOI: 10.1039/C9OB02085C

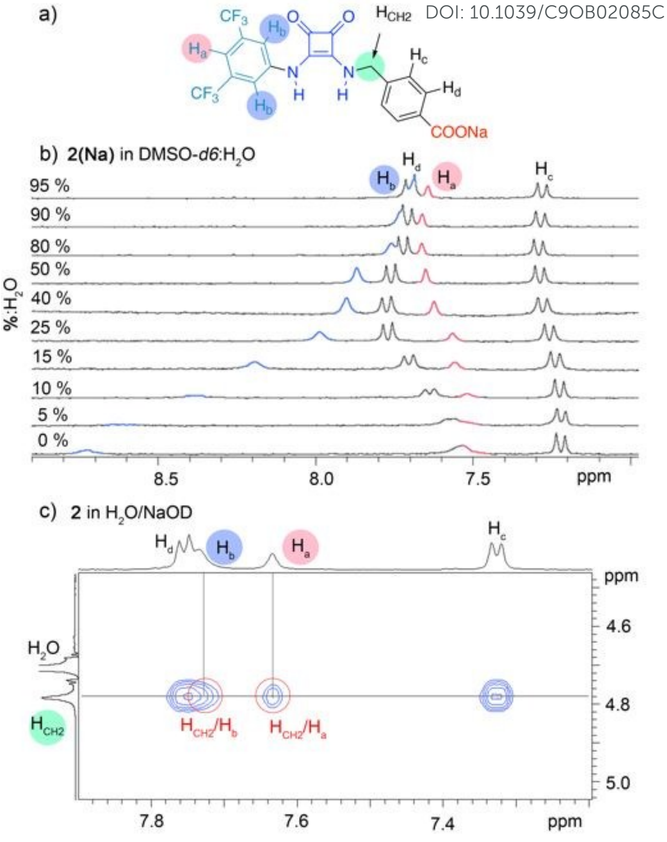

Fig. 4. a) Molecular structure of compound **2(Na)** and the labels of the distinct NMR protons. b) Stacked ^1H NMR spectra of **2**(Na) in H_2O:DMSO-*d6* mixtures (1.0×10^{-3} M). c) Relevant part of the NOESY spectrum of **2** in D_2O/NaOD (6.7×10^{-3} M).

Theoretical calculations

Experimental data results were supported by theoretical calculations. The self-assembled structures of squaramides **1** and **2** were theoretically investigated by using the Gaussian-09 software and the B3LYP-D/6-31+G* level of theory.[64] Initially, we optimized the monomeric species and obtained the molecular electrostatic potential MEP surfaces and then, dimeric structures were geometry optimized in order to figure out their aggregation model. Figs. 5a-b and S43 show the MEP surfaces and the dipole moment of the molecules alone. Remarkably, compounds **1** and **2** possess the largest dipole moments (10.1 and 8.5 D, respectively) of the **1-5** series (Table S1). Furthermore, while for compounds **3-5** the dipole moment is oriented perpendicular to the aryl-squaramide structure, in the case of **1** and **2** the direction of the vector is tilted along the

View Article Online
DOI: 10.1039/C9OB02085C

molecular axis. These features are determinant for the self-assembly behaviour (*vide infra*).

For the modelling of the dimeric structures (as model of supramolecular assembly) of compounds **1** and **2,** it was assumed that the benzoate groups are located at the periphery of the aggregates while the less polar arylsquaramide parts are located in the interior (Fig. 1b), according to the typical assembly of amphiphilic molecules in water.[14-19] Accordingly, simplified structures of **1** and **2** without the benzoate groups were utilized for the theoretical studies, in order to shorten the calculation time and avoid undesired interactions between squaramides and carboxylate groups. The dimeric structures were then geometry optimized, and the results are shown in Figs. 5c and S44. As shown for compound **2** (Fig. 5c), the dimer is formed by π–π interactions between the squaramide moiety and the 3,5-(bis(trifluoromethyl))phenyl rings while the dipole moments of the vicinal molecules are oriented in opposite directions and, consequently, the total dipole moment of the assembly is zero. Thus, the infinite stack of molecules *via* π–π dipolar interactions leads to the formation of 1D assemblies where the CO and NH groups of the squaramides point to the side of the aggregates. Analogous results were obtained for compound **1** (Fig. S44). We have also included two water molecules in the optimization (not shown in Fig. 5c) to model the experimental water environment. This interaction pattern agrees with the NOESY experiments that indicate that the methylene groups and the aryl groups of vicinal squaramidic compounds are proximal in the assembled structure. We believe that this interaction pattern combined with the hydrophobic effects drive the assembly of compounds **1** and **2** into 1D aggregates, that bundle forming fibers, as observed by AFM (Fig 2c,d).

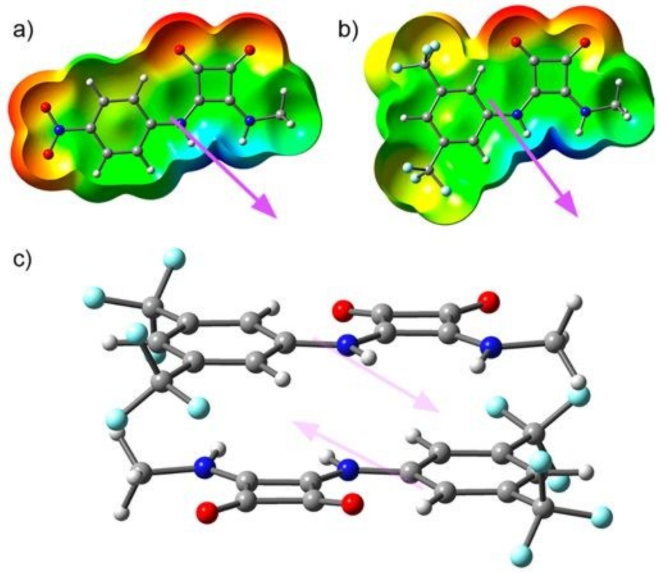

Fig. 5. Open MEP surfaces of compounds **1** (a) and **2** (b). Red and blue coloured isosurfaces represent negative and positive values of MEP. c) B3LYP-D/6-31+G* optimised dimer of compound 2. The dipole vectors are represented using pink arrows.

Experimental part

Preparation of gels and supramolecular polymers

The appropriate amount of **1** or **2** is suspended in few ml of mQ water, and the pH was set to 7.5-8 with PBS (or NaOH 0.1 M). Then the appropriate amount of additional mQ water is added until the desired concentration is reached. The mixture is heated to 80ºC for 1 hour and then solution is allowed to cool at room temperature. The samples prepared with NaOH requires 3-5 days to form gels (high concentrations) or reach the equilibrium (lower concentrations) however the samples prepared with PBS reach the equilibrium in 1-2 days after preparation.

Preparation of 1(Na) and 2(Na) salts

Compounds **1** and **2** were suspended in mQ water and a stochiometric amount of NaOH was added. The mixture was heated until everything is dissolved. Then the samples were cooled at r.t. and filtrated if appear a precipitate. Finally, solvent was removed by cold evaporation to give **1(Na)** and **2(Na)** as solids.

Theoretical calculations

The geometries of all compounds reported herein were fully optimized using the Gaussian-09 program[64] at the B3LYP[65]-D/6-31+G* level of theory. This level includes Grimme's dispersion correction that is adequate to study π-stacking assemblies.[66] The MEP surfaces and dipole moments have been computed at the same level of theory. The MEP surfaces have been represented using the 0.001 a.u. isosurface since it is the best estimate of the van der Waals surface. The minimum nature of the complexes has been confirmed by doing frequency calculations.

Conclusions

In this work we unveil a new interaction motif based on dipolar π–π interactions in squaramides **1** and **2** aggregates, which is distinct to the previously described hydrogen bonding and antiparallel stacking. Certainly, this is enabled by strong hydrophobic effects but also by the strong dipole moments in the arylsquaramide part with electron poor aryl rings. It might be highlighted that, while dipolar π–π interactions are well known in organic solvents, they are rarer in aqueous assemblies. We believe this discovery opens new strategies for the design of squaramide aggregates and which still have free squaramidic NHs groups suitable for the recognition of other species. Accordingly, and as we showed in our previous works, these squaramidic compounds are very attractive for the development of new aqua materials for drug delivery applications.

Conflicts of interest

There are no conflicts to declare.

Acknowledgements

We thank G. Martorell and J. Cifre of the SCT of the UIB for the technical support. We thank the MINECO/AEI (projects CTQ2017-85821-R and CTQ2017-90852-REDC, FEDER funds) for financial support. B. S. is thankful to the MINCIU and AEI for the Ayuda Ramón y Cajal (RYC-2017-21789) and the Govern de les Illes Balears (GOIB) for the AAEE 116/2017. S. B. and E. C. are thankful to SOIB and the Comunitat Autonoma de les Illes Balears for the financial support through the program "Joves Qualificats 2017".

View Article Online
DOI: 10.1039/C9OB02085C

Notes and references

‡ PBS (pH=7-8) is used as media in all the aggregation experiments to avoid variation on the pH and keep the benzoic acid group deprotonated.

§ The samples for the concentration dependent experiments were allowed to rest for 2 days. After this period no changes in the UV-Vis spectra were observed with time indicating that the thermodynamic equilibrium was reached.

§§ **1(Na)** and **2(Na)** were prepared from **1** and **2** by treatment with NaOH. The experimental details are described in the experimental part.

1. T. Aida, E. W. Meijer and S. I. Stupp, *Science*, 2012, **335**, 813-817.
2. L. Brunsveld, B. J. B. Folmer, E. W. Meijer and R. P. Sijbesma, *Chem. Rev.*, 2001, **101**, 4071-4097.
3. D. B. Amabilino, D. K. Smith and J. W. Steed, *Chem. Soc. Rev.*, 2017, **46**, 2404-2420.
4. S. S. Babu, V. K. Praveen and A. Ajayaghosh, *Chem. Rev.*, 2014, **114**, 1973-2129.
5. T. F. A. De Greef, M. M. J. Smulders, M. Wolffs, A. P. H. J. Schenning, R. P. Sijbesma and E. W. Meijer, *Chem. Rev.*, 2009, **109**, 5687-5754.
6. L. Yang, X. Tan, Z. Wang and X. Zhang, *Chem. Rev.*, 2015, **115**, 7196-7239.
7. C. Rest, R. Kandanelli and G. Fernandez, *Chem. Soc. Rev.*, 2015, **44**, 2573-2573.
8. J. Matern, Y. Dorca, L. Sánchez and G. Fernandez, *Angew. Chem. Int. Ed.*, 2019, DOI: 10.1002/anie.201905724
9. S. I. Stupp and L. C. Palmer, *Chem. Mater.*, 2014, **26**, 507-518.
10. M. Ogasawara, X. Lin, H. Kurata, H. Ouchi, M. Yamauchi, T. Ohba, T. Kajitani, T. Fukushima, M. Numata, R. Nogami, B. Adhikari and S. Yagai, *Mater. Chem. Front.*, 2018, **2**, 171-179.
11. S. Yagai, Y. Kitamoto, S. Datta and B. Adhikari, *Acc. Chem. Res.*, 2019, **52**, 1325-1335.
12. C. Rest, R. Kandanelli and G. Fernández, *Chem. Soc. Rev.*, 2015, **44**, 2543-2572.
13. V. Percec, D. A. Wilson, P. Leowanawat, C. J. Wilson, A. D. Hughes, M. S. Kaucher, D. A. Hammer, D. H. Levine, A. J. Kim, F. S. Bates, K. P. Davis, T. P. Lodge, M. L. Klein, R. H. DeVane, E. Aqad, B. M. Rosen, A. O. Argintaru, M. J. Sienkowska, K. Rissanen, S. Nummelin and J. Ropponen, *Science*, 2010, **328**, 1009-1014.
14. E. Krieg, M. M. C. Bastings, P. Besenius and B. Rybtchinski, *Chem. Rev.*, 2016, **116**, 2414-2477.
15. D. Gorl, X. Zhang and F. Wurthner, *Angew. Chem. Int. Ed.*, 2012, **51**, 6328-6348.
16. E. Krieg and B. Rybtchinski, *Chem. Eur. J.*, 2011, **17**, 9016-9026.
17. W. Li, Y. Kim, J. F. Li and M. Lee, *Soft Matter*, 2014, **10**, 5231-5242.
18. P. P. N. Syamala, B. Soberats, D. Görl, S. Gekle and F. Würthner, *Chem. Sci.*, 2019, **DOI:** 10.1039/C9SC03103K
19. C. M. A. Leenders, L. Albertazzi, T. Mes, M. M. E. Koenigs, A. R. A. Palmans and E. W. Meijer, *Chem. Commun.*, 2013, **49**, 1963-1965.
20. P. Besenius, G. Portale, P. H. H. Bomans, H. M. Janssen, A. R. A. Palmans and E. W. Meijer, *Proc. Natl. Acad. Sci.*, 2010, **107**, 17888-17893.
21. J. D. Hartgerink, E. Beniash and S. I. Stupp, *Science*, 2001, **294**, 1684-1688.
22. V. Grande, B. Soberats, S. Herbst, V. Stepanenko and F. Würthner, *Chem. Sci.*, 2018, **9**, 6904-6911.
23. H. Frisch, J. P. Unsleber, D. Lüdeker, M. Peterlechner, G. Brunklaus, M. Waller and P. Besenius, *Angew. Chem. Int. Ed.*, 2013, **52**, 10097-10101.
24. C. Rest, M. J. Mayoral, K. Fucke, J. Schellheimer, V. Stepanenko and G. Fernández, *Angew. Chem. Int. Ed.*, 2014, **53**, 700-705.
25. F. J. M. Hoeben, P. Jonkheijm, E. W. Meijer and A. P. H. J. Schenning, *Chem. Rev.*, 2005, **105**, 1491-1546.
26. Z. J. Chen, A. Lohr, C. R. Saha-Moller and F. Würthner, *Chem. Soc. Rev.*, 2009, **38**, 564-584.
27. A. Kaeser and A. P. Schenning, *Adv. Mater.*, 2010, **22**, 2985-2997.
28. S. S. Babu, V. K. Praveen and A. Ajayaghosh, *Chem. Rev.*, 2014, **114**, 1973-2129.
29. H. J. Kim, T. Kim and M. Lee, *Acc. Chem. Res.*, 2011, **44**, 72-82.
30. Z. S. Wang, J. J. Cui, Y. R. Liang, T. Chen, M. Lee, B. Z. Yin and L. Y. Jin, *J. Polym. Sci. A*, 2013, **51**, 5021-5028.
31. D. Görl, B. Soberats, S. Herbst, V. Stepanenko and F. Würthner, *Chem. Sci.*, 2016, **7**, 6786-6790.
32. D. Gorl, X. Zhang and F. Würthner, *Angew. Chem. Int. Ed.*, 2012, **51**, 6328-6348.
33. Fernández, F. García and L. Sánchez, *Chem. Commun.*, 2008, 6567-6569.
34. S. Ghosh and S. Ramakrishnan, *Angew. Chem. Int. Ed.*, 2004, **43**, 3264-3268.
35. A. Das and S. Ghosh, *Chem. Commun.*, 2011, **47**, 8922-8924.
36. A. Das and S. Ghosh, *Angew. Chem. Int. Ed.*, 2014, **53**, 2038-2054.
37. F. Würthner, *Acc. Chem. Res.*, 2016, **49**, 868-876.
38. F. Würthner, S. Yao and U. Beginn, *Angew. Chem. Int. Ed.*, 2003, **42**, 3247-3250.
39. S. Yao, U. Beginn, T. Gress, M. Lysetska and F. Würthner, *J. Am. Chem. Soc.*, 2004, **126**, 8336-8348.
40. G. Fernández, M. Stolte, V. Stepanenko and F. Würthner, *Chem. Eur. J.*, 2013, **19**, 206-217.
41. B. Soberats, L. Martinez, E. Sanna, A. Sampedro, C. Rotger and A. Costa, *Chem. Eur. J.*, 2012, **18**, 7533-7542.
42. C. Rotger, B. Soberats, D. Quinonero, A. Frontera, P. Ballester, J. Benet-Buchholz, P. M. Deya and A. Costa, *Eur. J. Org. Chem.*, 2008, 1864-1868.
43. J. Schiller, J. V. Alegre-Requena, E. Marqués-López, R. P. Herrera, J. Casanovas, C. Alemán and D. Díaz Díaz, *Soft Matter*, 2016, **12**, 4361-4374.
44. V. Saez-Talens, P. Englebienne, T. T. Trinh, W. E. M. Noteborn, I. K. Voets and R. E. Kieltyka, *Angew. Chem. Int. Ed.*, 2015, **54**, 10502-10506.
45. C. Tong, T. Liu, V. Saez Talens, W. E. M. Noteborn, T. H. Sharp, M. M. R. M. Hendrix, I. K. Voets, C. L. Mummery, V. V. Orlova and R. E. Kieltyka, *Biomacromolecules*, 2018, **19**, 1091-1099.
46. C. López, E. Sanna, L. Carreras, M. Vega, C. Rotger and A. Costa, *Chem. Asian J.*, 2013, **8**, 84-87.
47. R. Prohens, A. Portell, M. Font-Bardia, A. Bauzá and A. Frontera, *CrystEngComm*, 2016, **18**, 6437-6443.
48. R. Prohens, A. Portell, O. Vallcorba, M. Font-Bardia, A. Bauzá and A. Frontera, *CrystEngComm*, 2018, **20**, 237-244.
49. M. Ximenis, J. Pitarch-Jarque, S. Blasco, C. Rotger, E. García-España and A. Costa, *Cryst. Growth Des.*, 2018, **18**, 4420-4427.
50. L. A. Marchetti, L. Kumar Kumawat, N. Mao, J. C. Stephens and R. B. P. Elmes, *Chem*, 2019, **5**, 1398-1485.
51. C. López, M. Ximenis, F. Orvay, C. Rotger and A. Costa, *Chem Eur. J.*, 2017, **23**, 7590-7594.
52. A. Rostami, A. Colin, X. Y. Li, M. G. Chudzinski, A. J. Lough and M. S. Taylor, *J. Org. Chem.*, 2010, **75**, 3983-3992.
53. X. Ni, X. Li, Z. Wang and J.-P. Cheng, *Org. Lett.*, 2014, **16**, 1786-1789.
54. X. Du, J. Zhou, J. Shi and B. Xu, *Chem. Rev.*, 2015, **115**, 13165-13307.
55. F. Zhao, J. Bae, X. Zhou, Y. Guo and G. Yu, *Adv. Mater.*, 2018, **30**, 1801796.
56. A. S. Hoffman, *Adv. Drug Deliv. Rev.*, 2012, **64**, 18-23.

View Article Online
DOI: 10.1039/C9OB02085C

57 F. Rodríguez-Llansola, B. Escuder, J. F. Miravet, D. Hermida-Merino, I. W. Hamley, C. J. Cardin and W. Hayes, *Chem. Commun.*, 2010, **46**, 7960-7962.
58 R. Ian Storer, C. Aciro and L. H. Jones, *Chem. Soc. Rev.*, 2011, **40**, 2330-2346.
59 D. Quiñonero, A. Frontera, P. Ballester and P. M. Deyà, *Tet. Lett.*, 2000, **41**, 2001-2005.
60 J. Gershberg, F. Fennel, T. H. Rehm, S. Lochbrunner and F. Würthner, *Chem. Sci.*, 2016, **7**, 1729-1737.
61 N. L. Vekshin, *J. Biol. Phys.*, 1999, **25**, 339-354.
62 T. E. Kaiser, V. Stepanenko and F. Würthner, *J. Am. Chem. Soc.*, 2009, **131**, 6719-6732.
63 V. Saez Talens, D. M. M. Makurat, T. Liu, W. Dai, C. Guibert, W. E. M. Noteborn, I. K. Voets and R. E. Kieltyka, *Polym. Chem.*, 2019, **10**, 3146-3153.
64 M. J. Frisch, G. W. Trucks, H. B. Schlegel, G. E. Scuseria, M. A. Robb, J. R. Cheeseman, G. Scalmani, V. Barone, B. Mennucci, G. A. Petersson, H. Nakatsuji, M. Caricato, X. Li, H. P. Hratchian, A. F. Izmaylov, J. Bloino, G. Zheng, J. L. Sonnenberg, M. Hada, M. Ehara, K. Toyota, R. Fukuda, J. Hasegawa, M. Ishida, T. Nakajima, Y. Honda, O. Kitao, H. Nakai, T. Vreven, J. A. Montgomery, Jr., J. E. Peralta, F. Ogliaro, M. Bearpark, J. J. Heyd, E. Brothers, K. N. Kudin, V. N. Staroverov, R. Kobayashi, J. Normand, K. Raghavachari, A. Rendell, J. C. Burant, S. S. Iyengar, J. Tomasi, M. Cossi, N. Rega, J. M. Millam, M. Klene, J. E. Knox, J. B. Cross, V. Bakken, C. Adamo, J. Jaramillo, R. Gomperts, R. E. Stratmann, O. Yazyev, A. J. Austin, R. Cammi, C. Pomelli, J. W. Ochterski, R. L. Martin, K. Morokuma, V. G. Zakrzewski, G. A. Voth, P. Salvador, J. J. Dannenberg, S. Dapprich, A. D. Daniels, Ö. Farkas, J. B. Foresman, J. V. Ortiz, J. Cioslowski and D. J. Fox, Gaussian 09 (Gaussian, Inc., Wallingford CT, 2009).
65 (a) A. D. Becke, *J. Chem. Phys*., 1993, **98**, 5648-5652; (b) C. Lee, W. Yang and R. G. Parr, *Phys. Rev. B*, 1988, **37**, 785-789; (c) S. H. Vosko, L. Wilk and M. Nusair, *Can. J. Phys.* 1980, **58**, 1200-1211; (d) P. J. Stephens, F. J. Devlin, C. F. Chabalowski and M. J. Frisch, *J. Phys. Chem.*, 1994, **98**, 11623-11627.
66 S. Grimme, J. Antony, S. Ehrlich and H. Krieg, *J. Chem. Phys*., 2010, **132**, 154104.